Int. J. Heat Mass Transfer. Vol. 11, pp. 155–180. Pergamon Press 1968. Printed in Great Britain

TURBULENT MASS TRANSFER WITH AN ARBITRARY ORDER SURFACE REACTION IN A FLAT DUCT

CHARLES W. SOLBRIG and DIMITRI GIDASPOW
Institute of Gas Technology, IIT Center, Chicago, Illinois 60616, U.S.A.

(*Received* 3 *December* 1966 *and in revised form* 13 *July* 1967)

Abstract—Turbulent flow reactors with well-defined isothermal catalytic surfaces provide a method of obtaining rates of rapid surface processes. However, even in turbulent flow, diffusion tends to mask the true surface behavior at reasonable conversions of chemical species. To estimate the effect of diffusion on the rate of reaction, the Graetz problem for turbulent flow between parallel plates with an n-th order reaction on one wall has been solved.

Mixing cup concentrations were obtained for a range of Reynolds numbers of 30000–70000, Schmidt numbers 0·2–1·0, reaction orders of 1·0–2·0 and reaction rate constants from zero to infinity. The fully developed Nusselt numbers were approximately proportional to the 0·75 power of the Reynolds number and to the 0·65 power of the Schmidt number for the diffusion controlled cases. The fully developed Nusselt numbers were also somewhat dependent upon the reaction rate.

NOMENCLATURE

a, one half the distance between the catalytic and non-catalytic plate;
a_1, a_2, constants used to define turbulent flow region;
b_n, coefficients used in Wasan's analysis;
C, dimensionless concentration (weight fraction of reactant unconverted), $= \rho_a/\rho_{a0}$;
C_b, mixing-cup concentration;
C_w, concentration at the catalytic wall;
c_n, coefficient used in Wasan's analysis;
D_{ae}, effective diffusivity of species "a" in a mixture;
$D_t(y)$, eddy diffusivity of mass transfer;
d_n, coefficients used in Wasan's analysis;
F, friction factor;
f, velocity function, $= (v_y/1{\cdot}5\ U)$;
K_{w1}, dimensionless wall reaction rate constant for a first order reaction; Biot number for heat transfer;
K_{wn}, dimensionless wall reaction rate constant for an n-th order reaction, defined by equation (8);
K_E, effective dimensionless reaction rate constant;
k_c, mass-transfer coefficient defined by $D_{ae}\,\partial c/\partial y = k_c(C_b - C_w)$;
k_w, wall reaction rate constant [ft/h];
M_a, molecular weight of species "a";
Nu, Nusselt number for mass transfer, $k_c\,a/D_{ae}$;
O, order of magnitude;
Pe, Péclet number $= 4aU/D_{ae}$;
R, ratio used to define the turbulent center core;
R', the ratio $\Delta x/(\Delta s)^2$;
Re, Reynolds number based upon a distance "$2a$" between plates $= 4Ua\rho/\mu$;
Sc, Schmidt number $= \mu/\rho\,D_{ae}$;
s, normalized transformed distance $= s^+/s_0^+$;
s^+, transformed coordinate, $\mathrm{d}s = \mathrm{d}y/(1 + D_t/D_{ae})$;
s_0^+, distance in transformed coordinates corresponding to $y = 1$, defined by equation (27);
t^+, coordinate parameter, $= \theta v^*/\nu$;
U, mass average velocity;
v_i, mass velocity component in the i direction;

v^*, shear velocity, $= \sqrt{(\tau_w/\rho)}$;
v^+, dimensionless velocity, $= v/v^*$;
x, dimensionless coordinate parallel to flow, $= \eta/(\frac{3}{2} Ua^2/D_{ae})$;
y, dimensionless coordinate perpendicular to flow $= \xi/a$.

Greek symbols

α_1, ratio of eddy diffusivities of mass and momentum transfer;.
α_2, ratio of total diffusivities of mass and momentum transfer;
β_1, eigenvalue for the first mode;
ν, kinematic viscosity;
ϵ, eddy diffusivity of momentum;
θ, displaced coordinate, $\theta = \xi + a$;
η, spatial coordinate parallel to the flow direction;
μ, viscosity;
μ', eddy viscosity;
ξ, spatial coordinate perpendicular to the flow direction and the catalytic plate;
ρ, total density;
τ_w, shear stress at the wall;
ψ, function used in the finite difference equation solution, see equation (30).

Superscripts

$\bar{}$, barred quantities are used to denote time average quantities;
$'$, primed quantities are used to denote quantities fluctuating with time;
a^+, quantities with a superscript "+" and which are distances are defined $a^+ = a v^*/\nu$;
v^+, quantities with a superscript "+" and which are velocities are defined as $v^+ = v/v^*$.

INTRODUCTION

THE RATES of rapid surface reactions are best determined in a flow reactor. In order to avoid the masking of the true surface kinetics by diffusion it is often desirable to operate in the turbulent regime [1, 2]. Although rates of rapid surface reactions can be determined in tubular flow reactors, isothermal rectangular duct reactors with one well-defined catalytic wall are particularly advantageous because of the ease of assembly, inspection, and interchangeability of the catalytic surface. A flat rectangular duct reactor with a long adiabatic entrance section and one replaceable catalytic wall whose temperature can be maintained at the inlet gas temperature was built for this investigation. Analysis and experimental mass transfer and catalytic data were already presented for the laminar flow regime [3–7]. This paper gives a theoretical analysis of mass transfer with reaction on one wall of a flat rectangular duct reactor in the turbulent flow regime. The channel is sufficiently long to allow the velocity profile to become fully developed before the catalytic portion of the wall is reached. This fully developed velocity profile does not change in the catalytic section of the reactor, because the mass of reactants diffusing to the surface equals the mass of products diffusing away from the surface, the temperature remains constant and changes in total number of moles of the system are assumed to be small. The latter assumption will be exact for total combustion of methane or approximately true for combustion of most fuels in air where there is a large portion of inert gas. With these simplifying assumptions, all of which are easily realized in practice, the mass-transfer problem becomes analogous to the heat-transfer problem treated in the literature, except for the more general boundary conditions encountered in this study.

The solutions to this general problem under consideration have not been treated in the literature although certain cases have been treated extensively [8]. For example, the diffusion controlled case for flow in a tube as well as between parallel plates has been treated extensively. Due to the uncertainty in the actual form of the velocity and eddy diffusivity functions, the various analyses differ in their reported results by as much as 20 per cent.

Sparrow, Lloyd and Hixon [9] present a comparison between various analytical results. It is apparent that there are no "best" formulae for the velocity and diffusivity functions. The object of the literature survey conducted in this investigation was to determine formulae which will reproduce experimental measurements accurately within the range of Reynolds numbers of 30000 to 70000. The discussion of the selection of the velocity and diffusivity functions is better left to the later development sections.

After these functions have been selected, several different methods might be employed to solve the boundary value problem. These methods will be briefly described here and may be classified as: (1) the separation of variables analytical solution; (2) the separation of variables numerical solution; (3) the classical analogy approach; (4) the integral equation solution, and (5) the numerical solution of non-separable problems.

A work of Beckers [10] is an example of the solution to the problem in a tube by the analytical separation of variables technique. This involves separating variables and solving the equation in the direction of flow exactly. The equation perpendicular to the flow direction is solved by the method of Frobenius. Since the turbulent flow regime is defined in terms of separate regions (i.e. the laminar sublayer, the transition region, and the turbulent center region), a series solution is required in each of these regions. Equating the solutions and their derivatives at the boundaries of these regions and utilizing the boundary conditions completely specifies the eigenvalues and corresponding eigenfunctions.

The numerical separation of variables technique has been utilized by many investigators for pipe flow (see, for example, Sparrow, Hallman and Siegel [11] or Wissler and Schechter [12]). The method employed is similar to the previous with the exception that the separated equation perpendicular to the flow direction is solved numerically. Hatton and Quarmby [8] and Hatton [13] utilize this method to produce results particularly relevant to this study. They present results which can be compared to those obtained here for the diffusion controlled problem.

The classical analogy solution utilizes assumptions which allow considerable simplification in the solution (see, for example, Deissler [14] or Wasan and Wilke [15]). The conservation of species equation and the momentum equation are similar in the boundary layer and this fact is utilized in arriving at a solution. For this solution to be valid, the boundary conditions must also be similar and this restricts the solution to the diffusion controlled case. In addition, the solution does not consider a variation in the direction of flow so that the solution is valid only in the fully developed region. The generality of the boundary condition considered here makes this method inapplicable for present purposes.

Wissler and Schechter [12] present a method for solving the problem of turbulent flow in a tube by integral equations. The method is based upon the solution presented by Katz [16] for laminar flow with similar boundary conditions. In a similar manner as Katz, Wissler and Schechter report a solution in which a term arising from the discontinuity of the condition at $x = 0$ is missing. However, they use another form of the solution, which has this term remaining in it, to obtain numerical results. They compared the results they obtained by this method to results they obtained by the numerical separation of variables technique and noted agreement within 1 per cent. They reported results only for the first-order case. n-th order reactions would require solving a non-linear integral equation.

The numerical solution of the non-separable non-linear problem considered here has not been treated in the literature to the best of the authors' knowledge.

The last method is the only one which is used in the following developments. The separation of variables methods are applicable only to the first-order reaction so they could not

be used for the general problem. The analogy approach was not used because of its restricted applicability. The integral equation solution could be applied, however, it was decided to solve the problem numerically.

CONSERVATION OF SPECIES

The coordinates and geometry are shown in Fig. 1. A potentially reactive incompressible fluid flows from left to right between parallel plates with a fully developed turbulent velocity profile. The chemical reaction occurs only on the catalytic wall starting at $\eta = 0$. Any heat liberated or absorbed by the reaction is transferred through the catalytic wall thus maintaining the fluid at a constant temperature. It is assumed that molecular diffusion of species "a" can be described by an effective constant binary diffusivity, D_{ae} [17]. Analogously, an eddy diffusivity for mass transfer, D_t is introduced.

Conservation of species "a" at a steady state can be expressed [18] by the equation

$$\frac{\bar{v}_\eta}{\frac{3}{2}U}\frac{\partial \bar{\rho}_a}{\partial x} = \frac{1}{\frac{3}{8}Pe}\frac{\partial}{\partial x}\left(-\frac{a}{D_{ae}}\overline{\rho_a' v_\eta'} + \frac{1}{\frac{3}{8}Pe}\frac{\partial \bar{\rho}_a}{\partial x}\right) + \frac{\partial}{\partial y}\left[(D_t + D_{ae})\frac{\partial \bar{\rho}_a}{\partial y}\right] \quad (1)$$

where

$$x = \frac{\eta}{\frac{3}{2}Ua^2/D_{ae}} = \frac{1}{\frac{3}{8}Pe}\left(\frac{\eta}{a}\right), \quad y = \frac{\xi}{a} \quad (2)$$

and where ρ_a is the mass concentration of species a, $\bar{v}_\eta$ is the velocity in the η direction, U is the average velocity, the bar superscripts indicate time averaged quantities and the primes denote fluctuating quantities.

The first term on the right-hand side of the equation is usually neglected and this procedure will be adopted here. This seems reasonable since the Péclet number in turbulent flow is usually large. Schneider [19] has considered the problem of slug flow which indicates that, for Péclet numbers above 100, one may neglect this term.

This equation must then be solved subject to the following initial and boundary conditions. The inlet composition is uniform and equal to ρ_{a0}. At the non-catalytic wall the mass balance shows that the gradient of the mass concentration is zero. Net zero mass velocity at the catalytic wall yields the following balance for an n-th order reaction.

$$D_{ae}\frac{\partial \bar{\rho}_a}{\partial y} = M_a k_w \bar{C}_a^n. \quad (3)$$

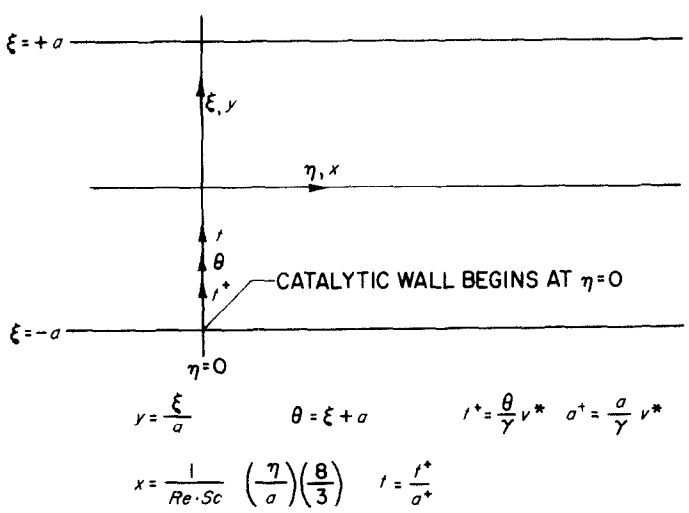

FIG. 1. Coordinates for the turbulent flow problem.

In equation (3), $\bar{C}_a$ is the molar concentration at the catalytic wall, k_w is the n-th order reaction rate constant and M_A is the molecular weight. No fluctuating components are included in this equation because the fluctuations decrease to zero at the wall.

Using the mass concentration of the feed as a scale factor for composition and neglecting molecular and eddy diffusion in the direction of flow, the boundary value problem becomes:

$$f(y)\frac{\partial C}{\partial x} = \frac{\partial}{\partial y}\left[\left(1 + \frac{D_t(y)}{D_{ae}}\right)\frac{\partial C}{\partial y}\right] \tag{4}$$

$$C(0, y) = 1 \tag{5}$$

$$\frac{\partial C}{\partial y}(x, 1) = 0 \tag{6}$$

$$\frac{\partial C}{\partial y}(x, -1) = K_{wn}[C(x, -1)]^n \tag{7}$$

where

$$K_{wn} = \frac{k_w a}{D_{ae}}\left(\frac{\rho_{a0}}{M_a}\right)^{(n-1)} \tag{8}$$

$$C = \frac{\bar{\rho}_a}{\rho_{a0}} \tag{9}$$

and

$$f = \frac{\bar{v}_\eta}{\frac{3}{2}U}. \tag{10}$$

The analogous heat-transfer problem is stated in [18].

VELOCITY PROFILES AND EDDY DIFFUSIVITIES

It is necessary to determine the velocity profile and the eddy diffusivity of mass transfer in order to completely specify the mass-transfer problem. The eddy diffusivity of mass transfer may be related to the eddy diffusivity of momentum ϵ by the relation

$$1 + \frac{D_t}{D_{ae}} = 1 + Sc\frac{D_t}{\epsilon}\frac{\epsilon}{\nu}. \tag{11}$$

The eddy diffusivity of momentum is in turn uniquely related to the velocity profile by the momentum equations. Therefore if a suitable form of D_t/ϵ is known, either from experiment or theory, the mass-transfer problem is completely specified when the velocity profile is determined. Frequently, D_t/ϵ is assumed to be equal to one. In this analysis, D_t/ϵ will be taken as a constant and results reported in terms of $Sc' = Sc \cdot D_t/\epsilon$ which allows a value of D_t/ϵ other than one to be used.

In order to use the universal velocity profile, a transformation must be made from real variables to "parameter variables". These are the shear velocity v^*, the velocity parameter v^+, and the coordinate parameter t^+ and are given by

$$v^* = \sqrt{\left(\frac{\tau_w}{\rho}\right)} \qquad v_\eta^+ = \frac{\bar{v}_\eta}{v^*} \qquad t^+ = \frac{\theta}{\nu}v^* \tag{12}$$

where τ_w is the shear stress at the wall and θ is the real distance from the wall. Once the functional form of the velocity parameter is determined by experiment, only the Reynolds number need be specified to completely determine the actual velocity and eddy diffusivity of momentum since

$$Re = \frac{4aU}{\nu} = 4\int_0^{a^+} \bar{v}_\eta^+ \, dt^+ \tag{13}$$

implicity determines the half distance

$$a^+ = \frac{a}{\gamma}v^*$$

which, in turn, specifies the average velocity U^+ by

$$Re = \frac{4aU}{\nu} = 4a^+ U^+. \tag{14}$$

It should be noted that the parameter variable half distance a^+ is a function of Reynolds number, even though, the actual half distance, of course, is not. The velocity function of equation (4) is specified by

$$f = \frac{\bar{v}_\eta}{\frac{3}{2}U} = \frac{\bar{v}_\eta^+}{\frac{3}{2}U^+}. \tag{15}$$

The eddy diffusivity of momentum is related to the velocity profile by the well known relation [18]

$$\frac{\epsilon}{\nu} = -\frac{\left(\frac{t^+}{a^+} - 1\right) + \frac{\partial \bar{v}_\eta^+}{\partial t^+}}{\frac{\partial \bar{v}_\eta^+}{\partial t^+}}. \tag{16}$$

It should be noted that the friction factor, F, is determined uniquely from the previous information by

$$F = \frac{2}{(U^+)^2} = 32\left(\frac{a^+}{Re}\right)^2. \tag{17}$$

Since friction factors are well known, equation (17) may be used as a check upon the velocity profile used in this analysis.

The velocity profiles used are based upon the work of several investigators. The experimental work reported in several articles by Corcoran, Page, Sage, Breaux, and Schlinger [20–24] is quite an extensive work and is used as the basis for selection of the constants used here in the universal velocity profile.

Prandtl hypothesized that the velocity parameter function vs. the distance parameter is the same function, the universal logarithmic velocity-distribution, for any Reynolds number. Experimental points obtained by Donch and Nikuradse [25] and described by the values $A = 6{\cdot}2$ and $B = 3{\cdot}6$ in the universal velocity profile.

$$\bar{v}_\eta^+ = A \log t^+ + B \tag{18}$$

where log is taken to the base 10.

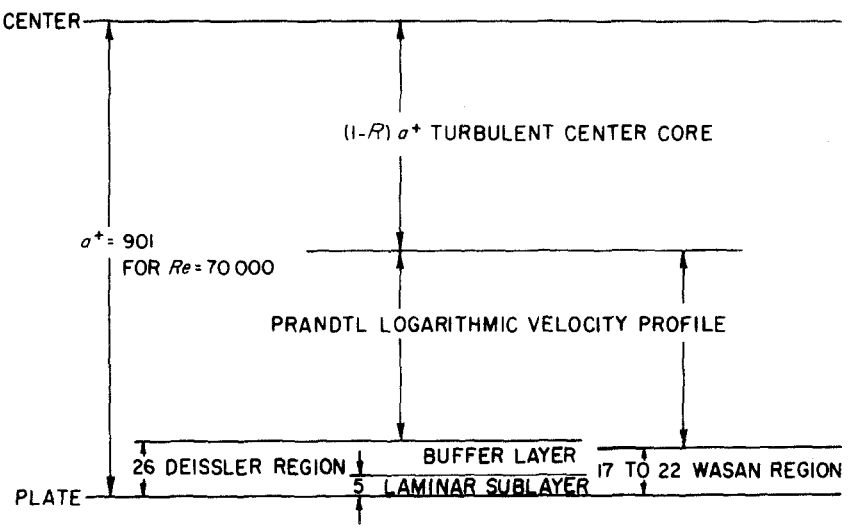

FIG. 2. Regions of turbulent flow.

The present study is restricted to turbulent flow between smooth parallel plates. Smooth plates are chosen so that the roughness factor need not be considered as an additional parameter in the results.

There are several inconsistencies with the use of the universal velocity profile. The velocity gradient being zero at the center cannot be described by this universal profile. A second fault is its value at the wall which indicates the

velocity is minus infinity rather than zero. The region near the wall is very difficult to measure because it corresponds to a very small physical distance. The description of the wall region has led to the hypothesis of a laminar sublayer next to the wall in which only laminar flow exists, and a buffer layer, which is a transition layer from the laminar sublayer to the region which can be described by the logarithmic profile. These regions are shown in Fig. 2. The fact that the velocity gradient is zero at the center has led to the hypothesis of another region, the turbulent center core in which the eddy diffusivity is constant. The laminar sublayer is generally taken to extend to a value of $t^+ = 5$. The buffer layer is presently taken to extend to a value of $t^+ = 26$. The turbulent center core is taken to extend from (Ra^+) to a^+. Different investigators have taken R to be 0·3 Wasan [26], 0·5 Hatton [13] and 0·66 Barrow [27]. Deissler improved the wall region description by combining the laminar and buffer region into one region [14]. However Deissler's formulation included a discontinuity in the derivative $d\bar{v}_\eta^+/dt^+$ between the Deissler region $(0 < t^+ < 26)$ and the Prandtl region $(26 < t^+ < Ra^+)$. Equation (16) shows that this implies that a discontinuity exists in the eddy diffusivity at that point. Wasan, Tien and Wilke *et al.* [28, 29] have presented a development in which the velocity parameter function is expanded about the wall. The series is truncated after five terms and the series and its first and second derivative are matched with the Prandtl logarithmic velocity profile at some distance, a_2^+. With this approach, a discontinuity does not exist. The width of the Wasan region a_2^+ depends upon the value of the constants in the logarithmic velocity profile but, in general, $17 \leqslant a_2^+ \leqslant 22$.

The third difficulty associated with the Prandtl velocity profile is that the "constants" are not constant but depend somewhat upon Reynolds number. This is substantiated by the data of Schlinger and Sage [24, 18]. Their data indicate that different constants must be used for different Reynolds numbers up to a Reynolds number of about 30000 but that the same constants may be used for any Reynolds number above this. Their data illustrate quite well that the velocity dips below the logarithmic velocity profile at the center. Although this deviation appears to occur only in a small region when plotted on semilog paper, this region actually corresponds to about half the distance between the plate and the center. Their data for higher Reynolds numbers agree well with the data presented by Nikuradse and Donch [25].

Hatton [13] has presented results similar to those of Corcoran *et al.* [21] but did not observe as large a variation in the velocity profile constants with Reynolds number. The constants used in this study were selected from the work of Hatton in the range of Reynolds number of 30000–70000. All of the various investigators agreed with Hatton's results in this range.

The universal velocity profile was used only in the Prandtl region. The expression for the velocity in the Wasan wall region was obtained by Wasan *et al.* [28] by series expansions about the wall. The derivation of this expression is included in [29]. The technique consists of expanding the quantities $\bar{v}_\eta$, v'_η, v'_ξ about the wall, applying the continuity and Navier–Stokes equations in the wall region, and equating the velocity, its first, and its second derivative to the universal profile at some point, a_2^+, near the wall. The location of this point and the coefficients of the expansion are determined by this technique.

The velocity in the turbulent center core is obtained by expanding the velocity about the center as

$$\bar{v}_\eta = \sum_0^\infty g_{2n}\xi^{2n}. \tag{19}$$

Only even powers are retained since the velocity must be symmetric about the center. No additional information is obtained by expanding the fluctuating velocities. If this function is

truncated after g_2, the function and its first and second derivative may be equated to the logarithmic profile at some distance a_1. If this is done and the results transformed to parameter coordinates, then

$$\bar{v}_\eta^+ = \bar{v}_{\eta^+ \max} + g_2^+(t^+ - a^+)^2$$
$$a_1^+ = \tfrac{1}{2}a^+ \tag{20}$$

$$v_{\eta^+ \max} = A\left(\ln\frac{a^+}{2} + \frac{1}{2}\right) + B$$
$$g_2 = -\frac{2A}{(a^+)^2}. \tag{21}$$

If the second derivatives are not required to be equal, equations (20) and (21) may be written to include an arbitrary ratio, R, of a_1^+ to a^+. That is

$$a_1^+ = Ra^+$$
$$\bar{v}_{\eta\max} = A\left[\ln(Ra^+) + \frac{(1-R)}{2R}\right] + B \tag{22}$$
$$g_2 = \frac{A}{2R(R-1)a^{+2}}.$$

The velocity profile in this region, equation (20), is in the form of a velocity defect profile since

$$\bar{v}_{\eta^+ \max} - \bar{v}_{\eta^+} = \frac{\bar{v}_{\eta\max} - \bar{v}_\eta}{v^*}$$
$$= -g_2^+(t^+ - a^+)^2. \tag{23}$$

Equation (16) may be used to determine the eddy diffusivity of momentum from the parameter velocity profiles. The results of the velocity and eddy diffusivity may be summarized as:

(1) Wasan wall region: $0 \leqslant t^+ \leqslant a_2^+$

$$\bar{v}_\eta^+ = t^+ + b_4^+(t^+)^4 + b_5^+(t^+)^5$$
$$\frac{\epsilon}{\nu} = -\frac{4b_4^+(t^+)^3 + 5b_5^+(t^+)^4}{1 + 4b_4^+(t^+)^3 + 5b_5^+(t^+)^4}$$
$$12a_2^+ + 9A - 20A\ln a_2^+ - 20B = 0$$
$$b_5^+ = -\frac{-4A + 3a_2^+}{5(a_2^+)^5}$$
$$b_4^+ = \frac{A - 5b_5^+(a_2^+)^5 - a_2^+}{4(a_2^+)^4}.$$

(2) Prandtl region: $a_2^+ \leqslant t^+ \leqslant a_1^+$ (24)

$$\bar{v}_\eta^+ = A\ln t^+ + B$$
$$\frac{\epsilon}{\nu} = \frac{t^+}{A}\left(1 - \frac{t^+}{a^+}\right) - 1.$$

(3) Turbulent center core: $a_1^+ \leqslant t^+ \leqslant a^+$

$$\bar{v}_\eta^+ = A\left[\ln(Ra^+) + \frac{(1-R)}{2R}\right] + B + \frac{A}{2R(R-1)}\left(\frac{t^+}{a^+} - 1\right)^2$$
$$\frac{\epsilon}{\nu} = \frac{R(1-R)}{A}a^+ - 1$$
$$a_1^+ = Ra^+.$$

If the second derivatives are required to be equal, $R = 0{\cdot}5$.

It should be noted that the parabolic velocity distribution in the turbulent center core implies that the eddy diffusivity is a constant in this region. Experimental evidence indicates that this is an approximation [22]. However, most investigators think that this is a good approximation and thus it will be accepted here.

The velocity profile constants were selected from the work of Hatton [13]. He apparently obtained these constants from the work of Schlinger and Sage [24] for Reynolds numbers above 35000. The values chosen were

$$A = 2{\cdot}777\ldots, \quad B = 3{\cdot}7923319, \quad R = 0{\cdot}5. \tag{25}$$

The values of A and B were judged to be correct by the authors because of the data of Schlinger and Sage [24]. The value of $R = 0{\cdot}5$ was chosen because this allowed the equating of the second derivatives at the boundary of the Prandtl and turbulent core regions. The value of 0·5 was also selected by Hatton. As stated previously, Barrow [27] has suggested that a value of $R = 0{\cdot}66$ be used. Figure 3 indicates that even when a value of $R = 0{\cdot}5$ is used, the parabolic profile coincides with the logarithmic

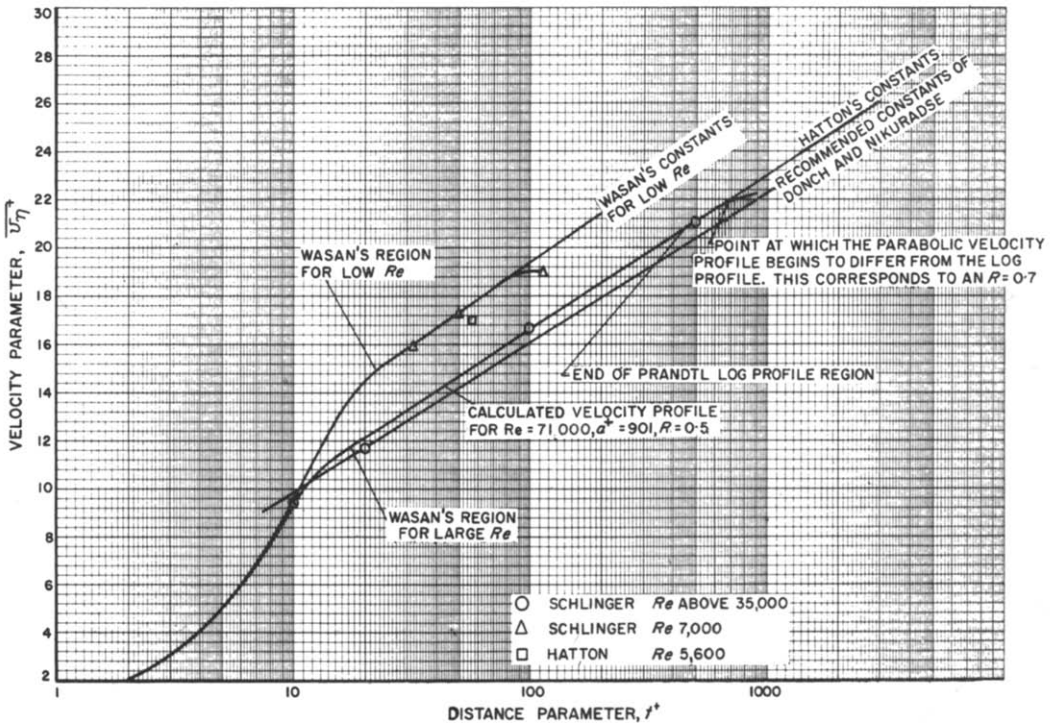

FIG. 3. Comparison of velocity profiles relevant to the present study.

profile to a value of $R = 0{\cdot}7$. Wasan [26] has suggested that a value of $R = 0{\cdot}3$ should be used in a tube. Replotting the velocity data in terms of a velocity defect on logarithmic paper indicates that the velocity defect is coincident with a straight line to a value of $R = 0{\cdot}3$. Therefore, it is concluded that the work of these three investigators is not in disagreement with respect to the velocity profile representation. Hatton, Quarmby and Grundy [30] investigated the effect of changing $R = 0{\cdot}5$ to $R = 0{\cdot}66$ in a problem involving heat transfer between parallel plates with one plate insulated. They state that "this modification, in fact, has a negligible effect on any of the heat transfer results".

The ratio of the eddy diffusivities of mass transfer to momentum is often assumed to be a constant equal to one. Some investigators have determined experimentally for the heat-transfer problem that this ratio could be as high as 1·6 [25]. For the purposes of analysis, this ratio need not be specified as long as it is a constant. Results can be reported in terms of ScD_t/ϵ and thus a greater generality in the results is obtained.

Azer and Chao [31, 32] presented expressions for calculating the ratio of eddy diffusivities of heat and momentum transfer which are based on experimental data. These expressions in the range

$$14000 < Re < 500000$$
$$0{\cdot}2 < Pr < 5$$

produce a small variation in D_t/ϵ of about 10 per cent from a distance of $t^+ = 0{\cdot}2a^+$ to a^+.

Nearer the wall, the variation is greater but the smaller eddy diffusivity of momentum tends to cancel this effect in calculating the eddy diffusivity of heat transfer. Although the method of analysis presented here is valid even if D_t/ϵ is a function of y, for definiteness and because it is a reasonable approximation, it will be assumed constant here

INTEGRAL TRANSFORMATION

The general statement of this problem, equations (4–7), dictate this problem to be non-separable due to the non-linear boundary condition. Direct application of a finite difference method is impractical because of the rapid change of velocity in the wall region. The subdivision in the y-direction would of necessity be of the order of 10^{-3} to include the laminar sub-layer. Although the increment size could be much larger near the center, the convergence of the finite difference method is controlled by the smallest subdivision in y. The increment of x which is required for convergence is of the order of $(\Delta y)^2$. Therefore it seems that a slightly different approach is called for. Accordingly, the integral transform is made

$$s^+ = \int_0^y \frac{dy}{[1 + (D_t/D_{ae})]} \tag{26}$$

where $1 + (D_t/D_{ae}) \to 1$ at the walls.
The distance from the center to the walls is given by

$$s_0^+ = \int_0^1 \frac{dy}{[1 + (D_t/D_{ae})]}. \tag{27}$$

Using the normalized integral transformation $s = s^+/s_0^+$ our differential system becomes, keeping in mind that D_t vanishes at the wall:

$$f(s)\frac{\partial C}{\partial x} = \frac{1}{[1+(D_t/D_{ae})](s_0^+)^2}\frac{\partial^2 C}{\partial s^2} \tag{28}$$

$$C(0, s) = 1$$

$$\frac{\partial C}{\partial s}(x, 1) = 0 \tag{29}$$

$$\frac{1}{s_0^+}\frac{\partial C}{\partial s}(x, -1) = K_{wn}[C(x, -1)]^n.$$

This integral transformation essentially expands the wall region. The transformation from y to s is shown in Fig. 4 for representative Reynolds and Schmidt numbers. This information was

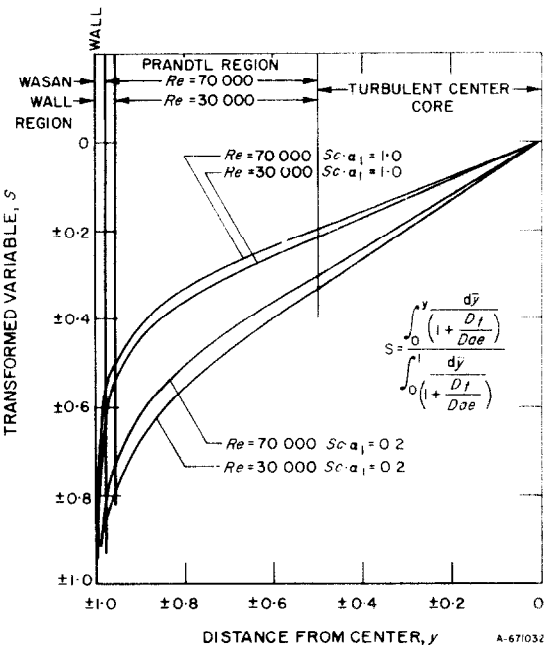

FIG. 4. Transformation of coordinates.

obtained by numerical integration and interpolation. With this information it is now possible to formulate a finite difference computational molecule.

FINITE DIFFERENCE SOLUTION

The application of the finite difference method of Dufort and Frankel [33] to equation (28)

results in the finite difference equation

$$C(I+1,J) = C(I-1,J) + \frac{2R'}{\psi + 2R'} \times [C(I,J+1) - 2C(I-1,J) + C(I,J-1)]$$

where

$$\psi = f(s) \cdot \left[1 + \frac{D_t(s)}{D_{ae}}\right] \cdot (s_0^+)^2$$

and

$$R' = \frac{\Delta x}{(\Delta s)^2}. \tag{30}$$

It should be noted that this is an explicit three grid computational molecule. It does not have the instability of the usual two grid molecule [18] or of the three grid Richardson molecule. The criterion of stability [33] is

$$0 < \frac{2R'}{\psi + 2R'} < 1. \tag{31}$$

This implies that ψ must be greater than zero and that the maximum value of ψ must be of the order of $2R'$. The function ψ is plotted in reference [18] for a Reynolds number near 70000. Although this function is zero only when $s = \pm 1{\cdot}0$, the value of ψ in the range $\pm(1{\cdot}0\text{–}0{\cdot}7)$ is near zero and is less than $0{\cdot}389 \times 10^{-4}$. Since the error in the calculations is slightly greater than this, divergence of the scheme is likely and in fact does occur. This leads to the necessity of a further refinement to the computational method. It is possible that the region in which $\psi < 0{\cdot}389 \times 10^{-4}$ one could assume as an approximation

$$\frac{\partial^2 C}{\partial s^2} = 0. \tag{32}$$

This would, however, lead to an uncomfortable position in deciding where one would switch from using equation (30) to equation (32). A much more satisfying solution was found by formulating the "double molecule" method. This refers to the use of two different computational molecules. The explicit method of Dufort and Frankel, equation (30), is used near the center where $\psi > 0$, and the completely implicit formulation is used near the walls. The implicit formulation is

$$C(I+1,J) = C(I,J) + R' \times \frac{[C(I+1,J+1) - 2C(I,J) + C(I+1,J-1)]}{(\psi + 2R')}. \tag{33}$$

This equation reduces to the finite difference formulation of the second derivative being zero near the wall, equation (32), if $\psi = 0$. The computational accuracy is not dependent upon which point the change is made between the two molecules as long as the implicit molecule is used when $\psi \approx 0$. However, the computer time increases the more that the implicit molecule is used because use of this molecule requires the inversion of a matrix. The order of this matrix equals the number of points it is used at. In actual computations, the number of points at which the implicit scheme was used was a variable dependent upon the Reynolds and Schmidt numbers. The implicit molecule was used at all points where $\psi < 0{\cdot}1\ \psi$ (max). Thus, a set of equations must be solved to obtain the concentrations at points near the catalytic wall and another set for points near the non-catalytic wall. Near the catalytic wall, one of the equations is non-linear since the boundary condition at the catalytic wall combined with the implicit molecule at points $(I+1, 2)$ yields the equation

$$C(I+1,2) + s_0^+ \Delta s\, K_{wn}\, C(I+1,2)^n - C(I+1,3) = 0. \tag{34}$$

The methods used to solve these equations is described in Appendix I.

In order to check the validity of this method, it was applied to the laminar flow case and the results were compared to our previous work on laminar flow [6]. The implicit molecule was used from the point next to the wall to $y = \pm \frac{1}{2}$

and the explicit molecule was used from $y = \pm\frac{1}{2}$ to the center. (In the laminar flow case, $y = s$.) The results obtained were the same (within roundoff error) as those obtained by using the method of Dufort and Frankel exclusively. Since $\psi = 0{\cdot}75$ at $y = \pm\frac{1}{2}$, it must be concluded that the point at which the change is made from one molecule to the other is irrelevant as long as the implicit molecule is used when $\psi \approx 0$. The accuracy of the scheme was checked in the turbulent flow case by comparing results obtained with twenty subdivisions in the s direction to those obtained with forty subdivisions in the s direction. Agreement between the two calculations was within one in the third decimal place. All reported calculations have been made with the smaller grid size.

The increment size Δx is related to Δs by the stability requirement that the maximum value of ψ must be of the same order as $2R$.

$$\Delta x = \frac{K}{2}(\Delta s)^2 \left\{ f(0)\left[1 + \frac{D_t(s)}{D_{ae}}\right](s_0^+)^2 \right\} \tag{35}$$

where $K = 1$ corresponds to equating $\psi(\max)$ and $2R$. In the laminar case this reduces to the familiar

$$\frac{\Delta x}{(\Delta y)^2} = \frac{K}{2}. \tag{36}$$

The accuracy is independent of K as long as K is in the range $0{\cdot}7 \leqslant K \leqslant 1{\cdot}3$. The value of K used in all the calculations was in this range.

The convergence of this scheme is illustrated in Appendix II. It is shown that equation (30) does converge to the differential equation as Δs approaches zero if Δx is related to Δs by equation (35).

OVERALL PARAMETERS

The mixing cup concentration may be expressed in s coordinates as

$$C_b = \frac{3}{4}\int_{-1}^{+1} C(x, s)\, f(s)\left[1 + \frac{D_t(s)}{D_{ae}}\right] s_0^+ \, \mathrm{d}s. \tag{37}$$

This was evaluated by use of Simpson's rule. The Nusselt number may be expressed in s coordinates as

$$Nu = \frac{\dfrac{1}{s_0^+}\dfrac{\partial C}{\partial s}(x, -1)}{C_b - C(x, -1)}. \tag{38}$$

For the first order case, it may be shown that

$$\frac{\partial C}{\partial y}(x, -1) = \left(\frac{1}{1/Nu + 1/K_{w1}}\right) C_b. \tag{39}$$

If the differential equation is integrated with respect to y, we obtain

$$\frac{\partial}{\partial x}\int_{-1}^{+1} f(y)\, C(x, y)\, \mathrm{d}y = \left(1 + \frac{D_t}{D_{ae}}\right)\frac{\partial C}{\partial y}\Bigg|_{(x,-1)}^{(x,+1)} \tag{40}$$

or when the boundary conditions are substituted, we obtain

$$\frac{\partial C_b}{\partial x} + \tfrac{3}{4}K_E\, C_b = 0 \tag{41}$$

where

$$K_E = \frac{1}{1/Nu + 1/K_{w1}}. \tag{42}$$

Equation (42) is the expression for an effective first order reaction rate coefficient. It illustrates the fact that when $K_{w1} \to \infty$, $K_E \to Nu$, the diffusion controlled case and when $K_w \to 0$, $K_E \to K_{w1}$, the reaction controlled case. This is the same expression as that obtained in laminar flow. Equation (42) illustrates that a much larger K_{w1} is needed to have a diffusion controlled reaction for laminar flow than turbulent. For example, in laminar flow, the fully developed Nusselt number in the diffusion controlled case is 1·215. A reaction rate of $K_{w1} = 50$ is sufficient to have a diffusion controlled reaction. For a Reynolds number of 30000 and $Sc' = 1{\cdot}0$, the fully developed, diffusion controlled Nusselt number is 28·6 and the required $K_{w1} > 1000$. Since the fully developed Nusselt number

increases with increasing Reynolds number (constant Sc'), reactions which are diffusion controlled at one Reynolds number are not at a higher Reynolds number in contrast to the laminar flow situation.

In [18], it is shown that the first-order turbulent flow case could have been solved by separation of variables. This forces the conclusion that for the first-order case, a fully developed solution exists and that K_E and Nu must approach a constant value given by

$$K_E = \frac{1}{1/K_w + 1/Nu} = \frac{\beta_1^2}{\frac{3}{4}} \tag{43}$$

where β_1 is the first eigenvalue.

RESULTS AND COMPUTATIONS

Rather extensive numerical computations were required to obtain results over the complete range of interest since four parameters are included in the statement of this problem. The four parameters include the dimensionless reaction rate coefficient, the reaction order, the Reynolds number, and the Schmidt number. Results were obtained for the diffusion controlled reaction for each combination of Reynolds numbers of 70000, 50000 and 30000 and Schmidt numbers of 1·0, 0·7 and 0·2. Results were also obtained for most of the combinations of dimensionless reaction rate constants of 10, 100, and 1000 and reaction orders of 1·0, 1·5,

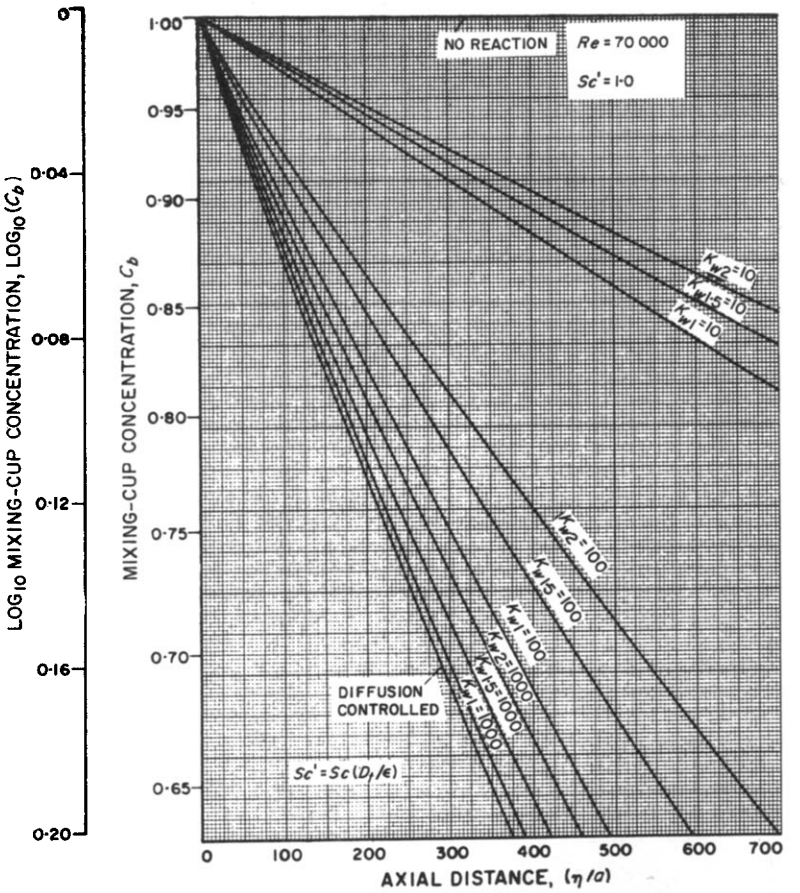

FIG. 5. Longitudinal concentration distribution—turbulent flow in a parallel plate duct with one catalytic plate—various reaction orders and constants.

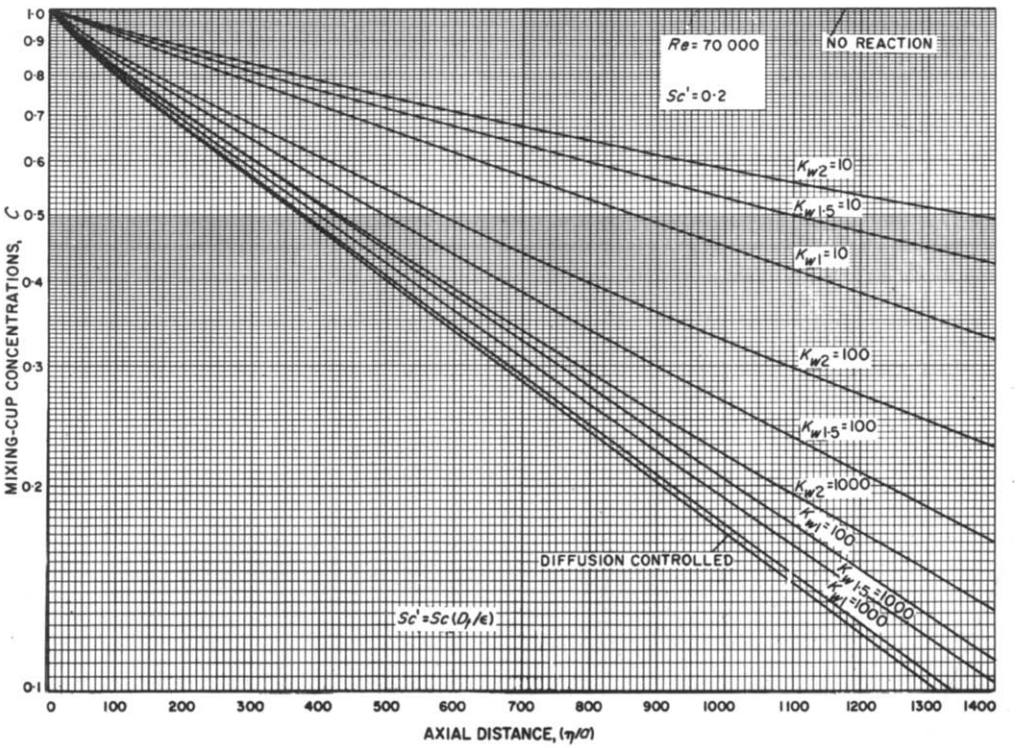

FIG. 6. Longitudinal concentration distribution—turbulent flow in a parallel plate duct with one catalytic plate—various reaction orders and constants.

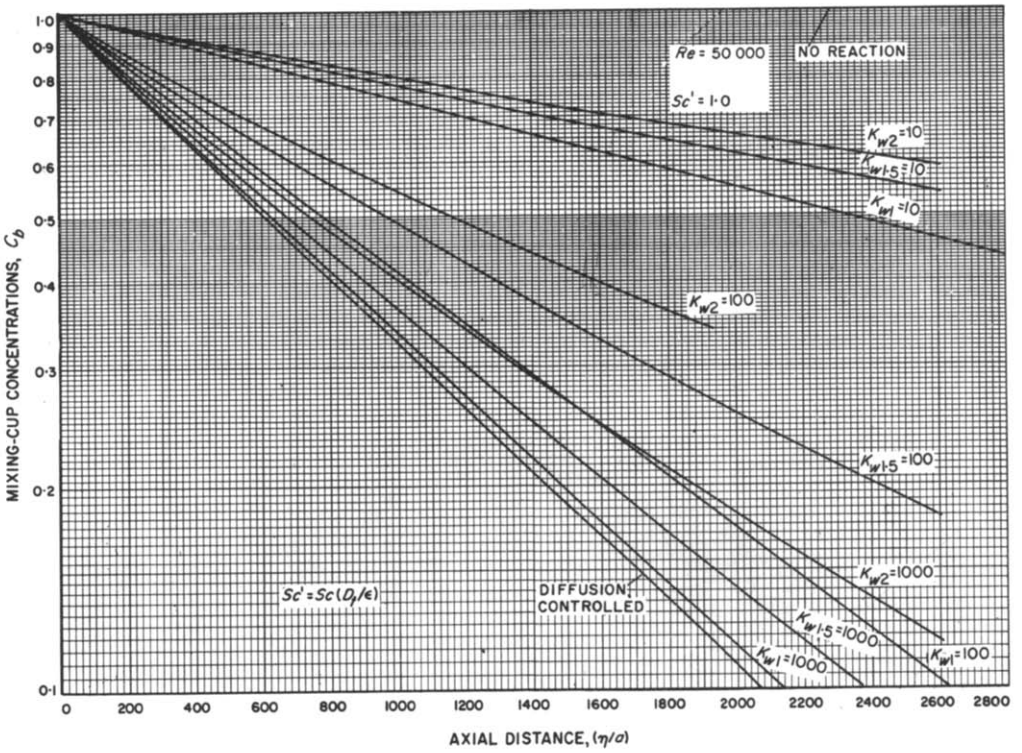

FIG. 7. Longitudinal concentration distribution—turbulent flow in a parallel plate duct with one catalytic plate—various reaction orders and constants.

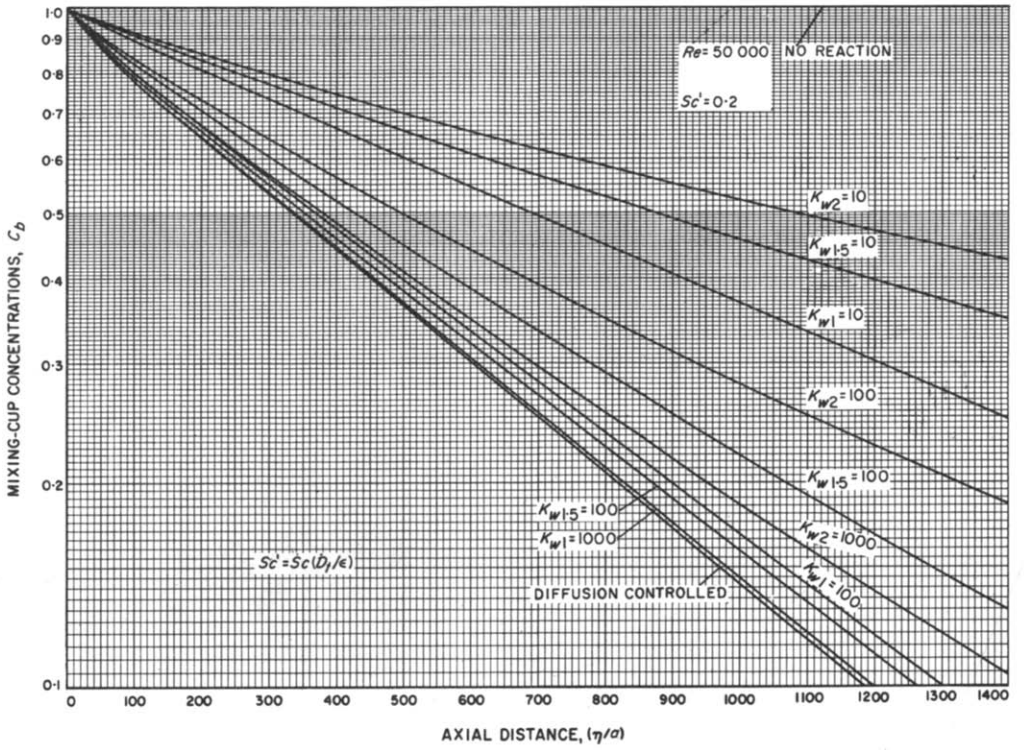

FIG. 8. Longitudinal concentration distribution—turbulent flow in a parallel plate duct with one catalytic plate—various reaction orders and constants.

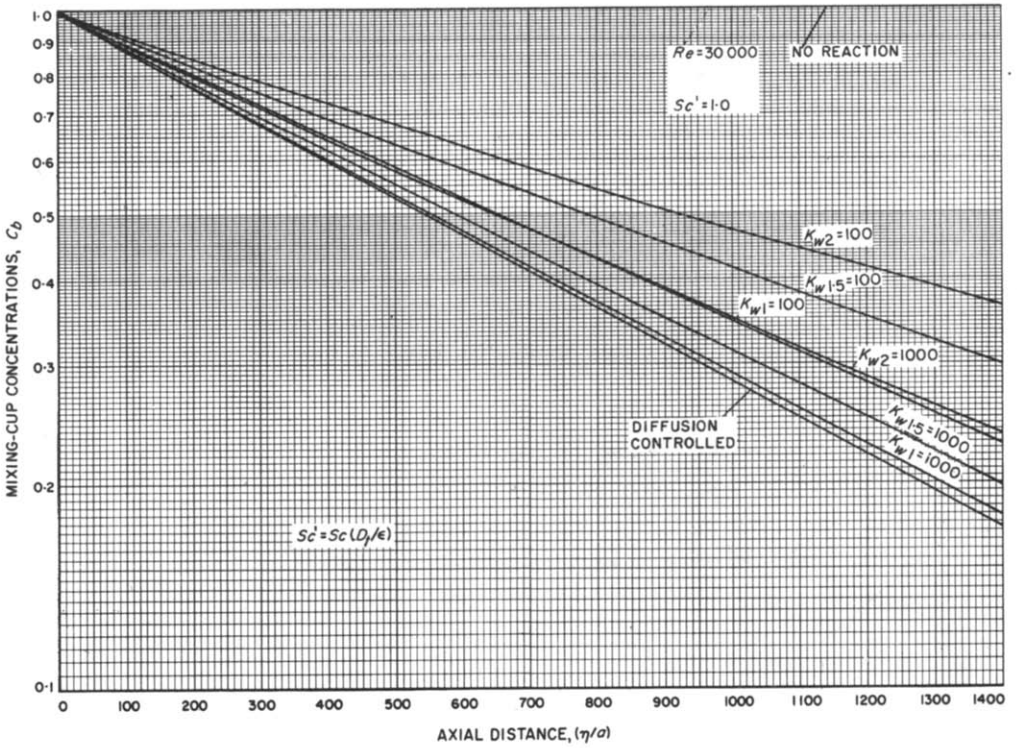

FIG. 9. Longitudinal concentration distribution—turbulent flow in a parallel plate duct with one catalytic plate—various reaction orders and constants.

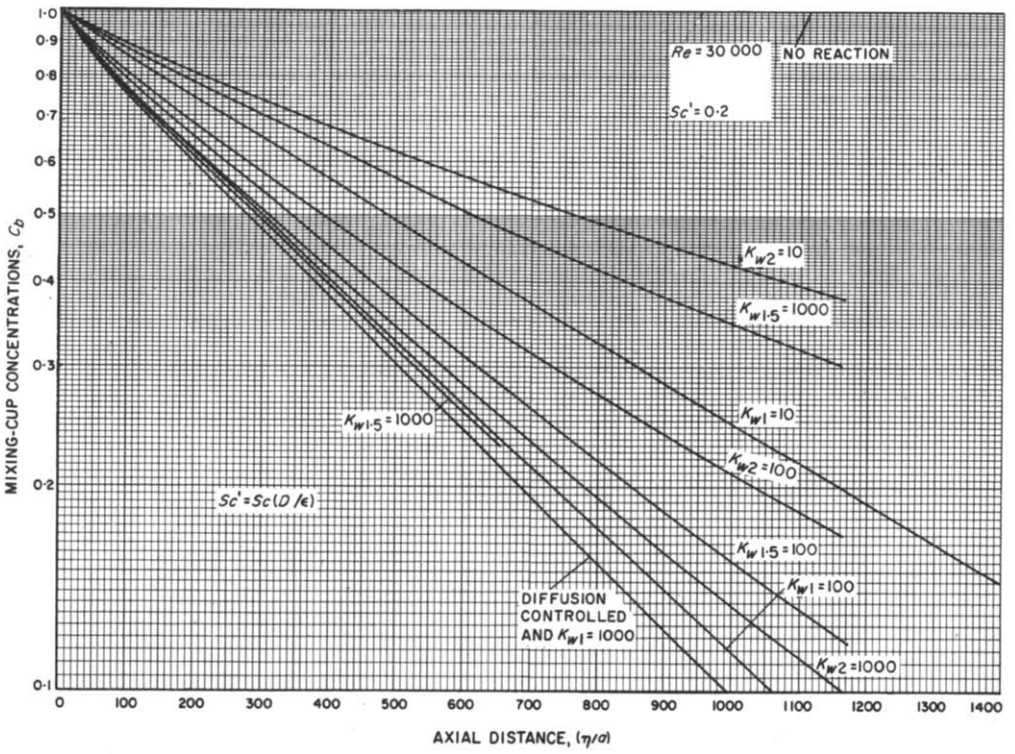

FIG. 10. Longitudinal concentration distribution—turbulent flow in a parallel plate duct with one catalytic plate—various reaction orders and constants.

and 2·0 for the Reynolds numbers and Schmidt numbers listed above.

Average concentration graphs are presented in Figs. 5–10. Schmidt numbers of 0·7 have not been included in these graphs because it was found experimentally that values of 0·7 could be obtained within two per cent by plotting C_b vs. the logarithm of Schmidt number for constant Re, η/a, n, and K_{wn}. The average concentration graphs presented are plotted on semi-log paper since all first order reactions should be straight lines on these coordinates in the fully developed region. All the diffusion controlled curves have been summarized in one graph in [6]. The diffusion controlled case is particularly useful in making estimations since the diffusion controlled reaction represents the minimum length a reactor must be to obtain a given conversion without knowing anything about the reaction rate. It is shown in [6] that the entrance length for the laminar concentration functions is greater than the entrance length for the turbulent concentrations. If the conversion of species "a" is plotted as a function of Reynolds number for a given value η/a, it appears that a discontinuity exists between the laminar and turbulent regimes in much the same manner as exists in a friction factor plot.

The average concentrations for diffusion controlled and first order reactions become straight lines for large values of x as predicted in [18] which shows the existence of a fully developed solution. Since the other average concentration graphs curve slightly, some of these curves intersect each other. The average concentration graphs should prove useful for

design purposes if the reaction rate is known. They can also be used to determine the true reaction rate from experimental data by interpolation as shown in [7].

As mentioned in [8], the reaction controlled reaction behaves in a manner similar to a one-dimensional homogeneous reaction. Figure 11 illustrates this point for the turbulent flow second order reaction. It is observed that as the dimensionless reaction rate constant is decreased, the reaction controlled average concentration function, F_n, becomes a straight line. The turbulent flow average concentration function for $K_{w2} = 10$ is essentially a straight line. The average concentration for laminar flow $K_{w2} = 10$ is included for comparison purposes and it is observed that it departs considerably from a straight line. This is expected since the given reaction rate is more likely to be diffusion controlled in laminar flow than turbulent flow.

The wall concentrations for a Reynolds number of 50000 and Schmidt number of 0·7 are illustrated in Fig. 12. The wall concentrations are larger than in the corresponding laminar case (see [18]).

The point concentration profiles for diffusion controlled reaction, $Re = 70000$ and $Sc = 1{\cdot}0$ are shown in Fig. 13. Concentration profiles were obtained for all the conditions for which average concentrations were obtained, however, only one of these is reported here. It is included to enable comparison of representative turbulent profiles to the profiles presented in the previous papers [3, 4] for laminar flow. It is noted that although this is a diffusion controlled reaction, the concentrations appear to be greater than zero at the wall. Actually they do decrease to zero in the boundary layer but the physical dimension of the boundary layer is so small that this cannot be observed. Experimental measurements of concentration profiles in turbulent flow with fast reactions can therefore not be

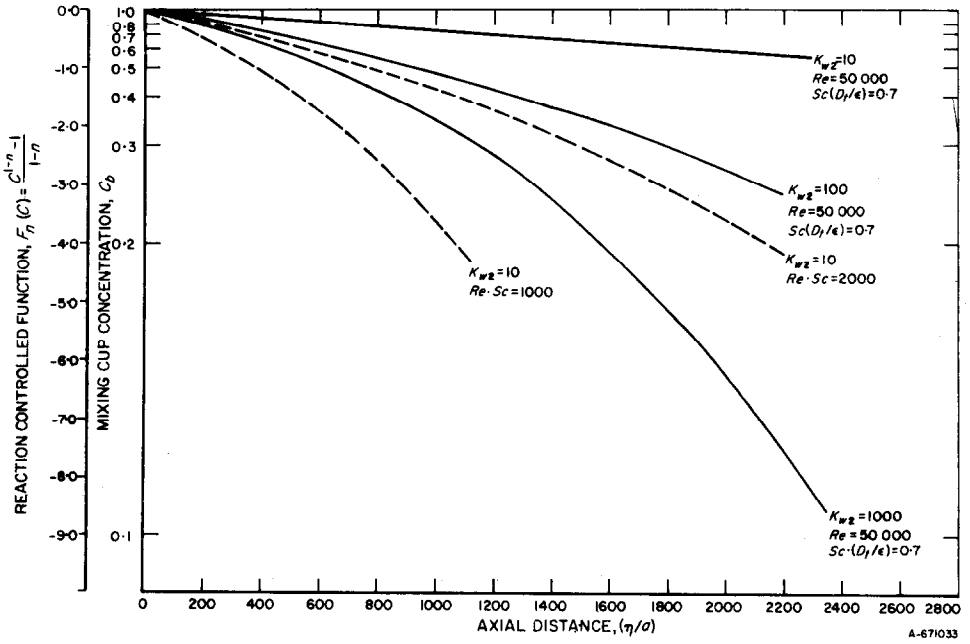

FIG. 11. Comparison of the masking of surface kinetics by convective diffusion in laminar and turbulent flow.

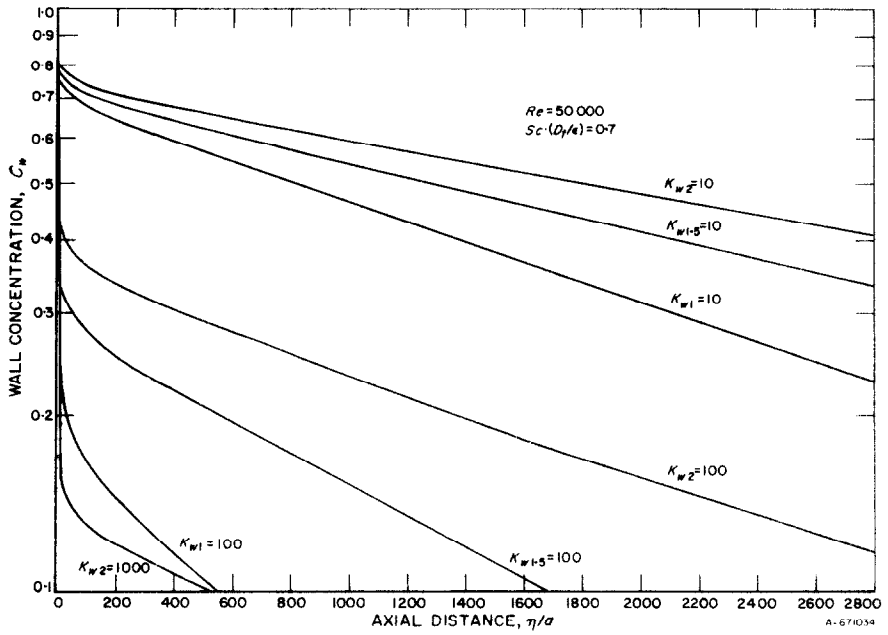

FIG. 12. Longitudinal wall distribution—turbulent flow in a parallel plate duct with one catalytic wall—various reaction orders and constants.

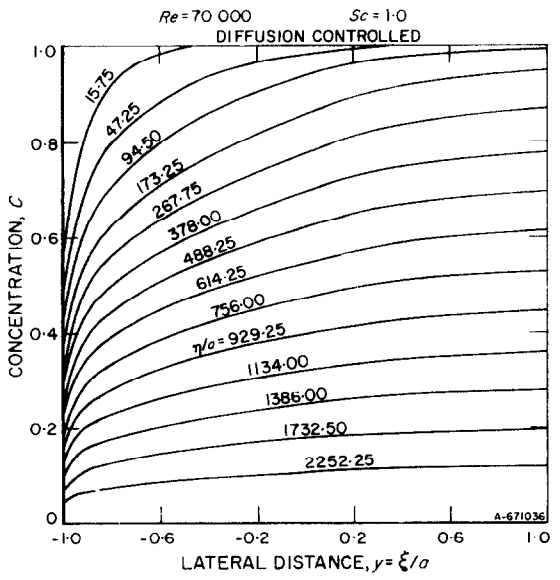

FIG. 13. Example of lateral concentration profiles—turbulent flow in a parallel plate duct with one catalytic wall.

used to determine the reaction rate. Since the boundary layer fills the entire duct in laminar flow, profiles may be used to determine reaction rates for fast reactions as shown in [4]. The accuracy of this method is enhanced by the fact that the concentration profile is a straight line for a considerable physical distance from the wall (see [3]).

It is observed in the preceding and in [6] that whenever laminar concentrations were compared to the turbulent concentrations for the same axial distance η/a and dimensionless reaction rate constant, the per cent conversion of species "a" is greater for the laminar case than for the turbulent. However, the total conversion of species "a" in a given amount of time is greater for the turbulent flow than for the laminar flow case.

The fully developed Nusselt number calculations are summarized in Fig. 14 for first order and diffusion controlled reactions on logarithmic paper. The slopes of the diffusion controlled

Nusselt number plotted as a function of Reynolds number varies between 0·77 for a Schmidt number of one and 0·69 for a Schmidt number of 0·2. These values compare to a value of 0·8 as predicted by the Dittus–Boelter equation. A variation in this slope with Schmidt number was also observed by Sparrow, Hallman and Siegel [11] in their analysis of convective diffusion with a constant flux boundary condition (hence equivalent to a zero order reaction) in a round tube. They reported a value of 0·77 for a Schmidt number of 1·0 which compares to 0·75 as determined in this work. The Nusselt number functions for Schmidt numbers of 1·0 and 0·7 exhibit the same slopes for the reaction rate coefficients of $K_{w1} = 10$ and 100.

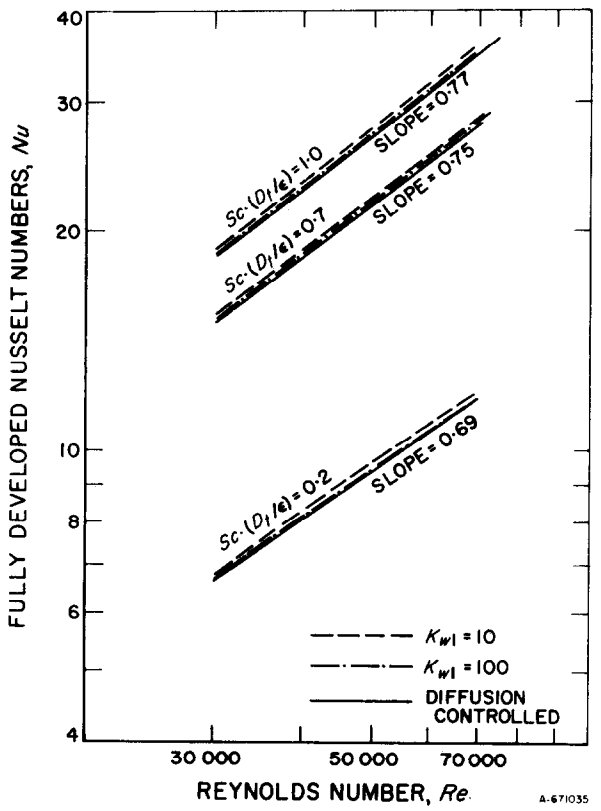

FIG. 14. Calculated mass-transfer correlations for the diffusion controlled and first order reactions.

In contrast, the reaction rate coefficients of $K_{w1} = 10$ and 100 produce slightly curved lines for a Schmidt number of 0·2.

Hatton and Quarmby [8] have calculated the Nusselt number for the diffusion controlled reaction for a Reynolds number of 73612 and a Schmidt number of one. Slight extrapolation of the results presented in Fig. 14 indicate a Nusselt number of 36·8 which compares to the value reported by Hatton, $Nu = 37{\cdot}05$. This is the only value he reports which may be compared directly because of the range of numbers he considered, however, even extrapolated values agree quite well. This agreement is particularly significant since Hatton used Deissler's wall region analysis rather than the analysis of Tien and Wasan [29] used here.

The fully developed diffusion-controlled Nusselt numbers have been replotted in [18] as a function of Schmidt number times the diffusivity ratio. The slopes of these graphs range from 0·69 to 0·61 for Reynolds numbers of 70000 and 30000 respectively. Assuming that the diffusivity ratio is one, one might expect these values to compare to values of 0·4–0·3 for the Dittus–Boelter equation. However, the Dittus–Boelter equation is used for a symmetric problem whereas the problem under consideration is unsymmetric.

Sparrow, Hallman and Siegel [11] investigated a much larger range of Schmidt numbers for flow in a tube and determined that Nusselt number could not be represented as a power function of Schmidt number. A power function representation is possible here because of the smaller range of Schmidt numbers.

The fully developed Nusselt number has been plotted as a function of the reaction rate coefficient for a Schmidt number of 1·0 and Reynolds number of 50000 in Fig. 15. The Nusselt number for the n-th order reaction essentially approaches a constant value for large values of η/a for the turbulent flow problem as well as for the laminar case. Thus fully developed Nusselt numbers are also included for the n-th order reaction in these

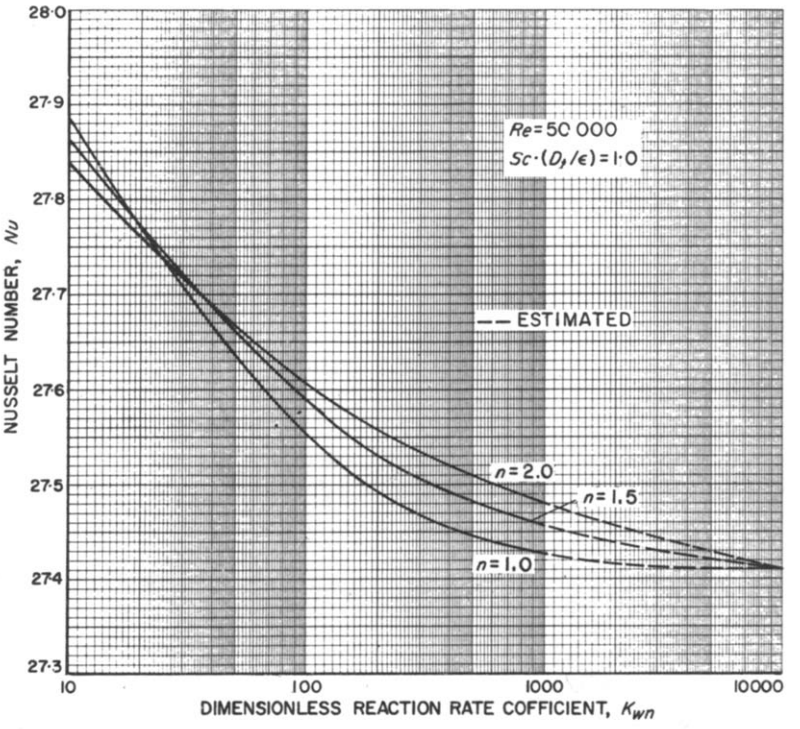

FIG. 15. Effect of heterogeneous chemical reactions on the mass-transfer coefficient for several reaction orders—turbulent flow.

figures. It is interesting to note that these curves intersect each other within a small range of K_{wn}. This range of intersection varies with Reynolds and Schmidt numbers.

CONCLUSIONS

The Graetz problem for turbulent flow between parallel plates with an n-th order reaction on one wall has been solved by a new method. The method includes an integral transformation of the convective diffusion equation, followed by an application of a double molecule finite difference scheme.

Rather extensive numerical results were obtained in order to cover the range of interest of Reynolds number, Schmidt number, and reaction rate. The important engineering information presented consists of mixing cup concentrations for reaction orders of 1·0, 1·5 and 2·0 which includes a large portion of reactions of industrial interest.

The standard definition of the Nusselt number was used here. The Nusselt number for the first order reaction approached a constant fully developed value for large values of x. The Nusselt number in the 1·5 and 2·0 orders essentially approached a constant value for large values of x.

The fully developed Nusselt numbers were approximately proportional to the 0·75 power of Reynolds number and to the 0·65 power of Schmidt number.

ACKNOWLEDGEMENT

This investigation was supported through the basic research program of the Institute of Gas Technology, supported by its members and contributors.

REFERENCES

1. D. GIDASPOW and R. T. ELLINGTON, Surface combustion of hydrogen: Part I. On platinum-coated alumina, *A.I.Ch.E. Jl* **10**, 707–713 (1964).
2. D. GIDASPOW and R. T. ELLINGTON, Surface combustion of hydrogen: Part II. On oxidized nickel, *A.I.Ch.E. Jl* **10**, 714–716 (1964).
3. C. W. SOLBRIG and D. GIDASPOW, Convective diffusion in a parallel plate duct with one catalytic wall—laminar flow—first order reaction—Part I—analytical, *Can. J. Chem. Engng* **45**, 35–39 (1967).
4. F. A. KULACKI and D. GIDASPOW, Convective diffusion in a parallel plate duct with one catalytic wall—laminar flow—first order reaction—Part II—experimental, *Can. J. Chem. Engng* **45**, 72–78 (1967).
5. C. W. SOLBRIG and D. GIDASPOW, Convective diffusion in a rectangular duct with one catalytic wall—laminar flow—arbitrary reaction order, *A.I.Ch.E. Jl* **13**(2), 346–351 (1967).
6. C. W. SOLBRIG and D. GIDASPOW, Convective diffusion in a parallel plate reactor with one catalytic wall—laminar flow—arbitrary reaction order, in the *Symposium of the 36th Congres International de Chimie Industrielle,* Bruxelles, 10–21 September (1966).
7. F. A. KULACKI, D. GIDASPOW and C. W. SOLBRIG, Analysis of *n*-th order reaction rate data using mixing cup charts, in the *Symposium of the 36th Congres International de Chimie Industrielle,* Bruxelles, 10–21 September (1966).
8. A. P. HATTON and A. QUARMBY, The effect of axially varying and unsymmetrical boundary conditions on heat transfer with turbulent flow between parallel plates, *Int. J. Heat Mass Transfer* **6**, 903–914 (1963).
9. E. M. SPARROW, J. R. LLOYD and C. W. HIXON, Experiments on turbulent heat transfer in an asymmetrically heated rectangular duct, *J. Heat Transfer* **88**, 170–174 (1966).
10. H. L. BECKERS, Heat transfer in turbulent tube flow, *Appl. Scient. Res.* **A6**, 147–190 (1956).
11. E. M. SPARROW, T. M. HALLMAN and R. SIEGEL, Turbulent heat transfer in the thermal entrance region of a pipe with uniform heat flux, *Appl. Scient. Res.* **A7**, 37–52 (1959).
12. E. H. WISSLER and R. S. SCHECHTER, Turbulent flow of gas through a circular tube with chemical reaction at the wall, *Chem. Engng Sci.* **17**, 937–948 (1962).
13. A. P. HATTON, Heat transfer in the thermal entrance region with turbulent flow between parallel plates at unequal temperatures, *Appl. Scient. Res.* **A12**, 249–266 (1963/64).
14. R. G. DEISSLER, Analysis of turbulent heat transfer, mass transfer, and friction in smooth tubes at high Prandtl and Schmidt numbers, NACA report 1210 (1955).
15. D. T. WASAN and C. R. WILKE, Turbulent exchange of momentum, mass, and heat between fluid streams and pipe wall, *Int. J. Heat Mass Transfer* **7**, 87–94 (1964).
16. S. KATZ, Chemical reactions catalyzed on a tube wall, *Chem. Engng Sci.* **10**, 202–211 (1959).
17. R. B. BIRD, W. E. STEWART and E. N. LIGHTFOOT, *Transport Phenomena.* John Wiley, New York (1960).
18. C. W. SOLBRIG, Convective diffusion in a rectangular duct with one catalytic wall, Unpublished Ph.D. Thesis, Illinois Institute of Technology, Chicago (1966).
19. P. J. SCHNEIDER, Effect of axial fluid conduction on heat transfer in the cntrance regions of parallel plates and tubes, *Trans. Am. Soc. Mech. Engrs* **79**, 765–773 (1957).
20. W. H. CORCORAN and B. H. SAGE, Role of eddy conductivity in thermal transport, *A.I.Ch.E. Jl* **2**, 251–259 (1956).
21. W. H. CORCORAN, F. PAGE, JR., W. G. SCHLINGER and B. H. SAGE, Temperature gradients in turbulent gas streams, *Ind. Engng Chem.* **44**, 410–419 (1952).
22. F. PAGE, JR., W. H. CORCORAN, W. G. SCHLINGER and B. H. SAGE, Temperature and velocity distributions in uniform flow between parallel plates, *Ind. Engng Chem.* **44**, 419–424 (1952).
23. F. PAGE, JR., W. G. SCHLINGER, D. K. BREAUX and B. H. SAGE, Point values of eddy conductivity and viscosity in uniform flow between parallel plates, *Ind. Engng Chem.* **44**, 424–430 (1952).
24. W. G. SCHLINGER and B. H. SAGE, Velocity distribution between parallel plates, *Ind. Engng Chem.* **45**, 2636–2639 (1953).
25. J. G. KNUDSEN and K. L. KATZ, *Fluid Dynamics and Heat Transfer.* McGraw-Hill, New York (1958).
26. D. T. WASAN, Analysis of gas phase mass transfer in turbulent flows, Unpublished Ph.D. Thesis, University of California, Berkeley (1964).
27. H. BARROW, An analytical and experimental study of turbulent gas flow between two smooth parallel walls with unequal heat fluxes, *Int. J. Heat Mass Transfer* **5**, 469–489 (1962).
28. D. T. WASAN, C. L. TIEN and C. R. WILKE, Theoretical correlation of velocity and eddy viscosity for flow close to a pipe wall, *A.I.Ch.E. Jl* **9**, 567–579 (1963).
29. C. L. TIEN and D. T. WASAN, Law of the wall in turbulent channel flow, *Physics Fluids* **6**, 144–145 (1963).
30. A. P. HATTON, A. QUARMBY and I. GRUNDY, Further calculations on the heat transfer with turbulent flow between parallel plates, *Int. J. Heat Mass Transfer* **7**, 817–823 (1964).
31. N. Z. AZER and B. T. CHAO, A mechanism of turbulent heat transfer in liquid metals, *Int. J. Heat Mass Transfer* **1**, 121–138 (1960).
32. N. Z. AZER and B. T. CHAO, Turbulent heat transfer in liquid metals—fully developed pipe flow with constant wall temperature, *Int. J. Heat Mass Transfer* **3**, 77–83 (1961).
33. E. C. DUFORT and S. P. FRANKEL, Stability conditions in the numerical treatment of parabolic differential equations, *Math Tab. Natn. Res. Coun., Wash.* **7**, 135–152 (1953).

APPENDIX I

The equations to be solved near the catalytic wall, equation (33) may be written as

$$EL(K, J)\, C(I + 1, J) = RES(K) + RIS(K)\, C(I, 2) \tag{I.1}$$

where EL, RES, and RIS are a matrix and two column vectors given by

$$EL = \begin{vmatrix} -\left[\frac{\psi(3)}{R} + 2\right] & 1 & 0 & 0 \\ 1 & -\left[\frac{\psi(4)}{R} + 2\right] & 1 & 0 \\ 0 & 1 & -\left[\frac{\psi(5)}{R} + 2\right] & 1 \\ 0 & 0 & 1 & -\left[\frac{\psi(6)}{R} + 2\right] \end{vmatrix}$$

$$RES = \begin{vmatrix} -\frac{\psi(3)}{R} C(I, 3) \\ -\frac{\psi(4)}{R} C(I, 4) \\ -\frac{\psi(5)}{R} C(I, 5) \\ -\frac{\psi(6)}{R} C(I, 6) \end{vmatrix} \qquad RIS = \begin{vmatrix} -1 \\ 0 \\ 0 \\ 0 \end{vmatrix}.$$

Solving

$$C(I + 1, J) = EL^{-1}(K, J)\, RES(K) + EL^{-1}(K, J)\, RIS(K)\, C(I + 1, 2). \tag{I.2}$$

Substituting $J = 3$ and combining with the non-linear boundary condition, equation (34), one must solve

$$[I - EL^{-1}(K, 3)\, RIS(K)]\, C(I + 1, 2) + s_0^+\, \Delta s K_{wn}[C(I + 1, 2)]^n - EL^{-1}(K, 3)\, RES(K) = 0. \tag{I.3}$$

After solving this equation for $C(I + 1, 2)$, equation (36) may be used to determine all the other $C(I + 1, J)\, 3 \leqslant J \leqslant 6$. A similar analysis is applied to the points from eighteen to twenty-one near the non-catalytic wall which is solved quite easily since the boundary condition there is linear. It is readily seen that if the implicit molecule is applied to more points, the size of the matrices which must be inverted become larger. In actual computations, the number of points at which the implicit molecule was applied was a variable and depended on the Reynolds and Schmidt number. The number of subdivisions used was forty instead of twenty.

APPENDIX II

The convergence of the computational molecule may be investigated by expanding the finite difference equation in a Taylor series and dropping the higher terms. This results in the equation

$$f\frac{\partial C}{\partial x} - \frac{1}{[1 + (D_t/D_{ae})](s_0^+)^2}\frac{\partial^2 C}{\partial s^2} = -f\frac{\Delta x^2}{6}\frac{\partial^3 C}{\partial s^3} + \frac{1}{[1 + (D_t/D_{ae})](s_0^+)^2}\left[\frac{\Delta s^2}{12}\frac{\partial^4 C}{\partial s^4} - \underline{\left(\frac{\Delta x}{\Delta s}\right)^2\frac{\partial^2 C}{\partial x^2}} - \frac{1}{12}\frac{\Delta x^4}{\Delta s^2}\frac{\partial^4 C}{\partial s^4}\right]. \quad \text{(II.1)}$$

Substitution of equation (35) into equation (II.1) indicates that all terms on the right-hand side of this equation approach zero as Δs approaches zero. However, this is not obvious for the underlined term. Consider, that the coefficient of $\partial^2 C/\partial x^2$ is

$$\frac{[(K/2)(\Delta s)^2 f(s)\{1 + [D_t(0)/D_{ae}]\}(s_0^+)^2]}{[1 + (D_t/D_{ae})](s_0^+)^2(\Delta s)^2} \leqslant M\,\Delta s^2 \quad \text{(II.2)}$$

where M is the maximum value

$$M = \max\left|\frac{1}{[1 + (D_t/D_{ae})](s_0^+)^2}\left[\frac{K}{2}f(s)\left(1 + \frac{D_t}{D_{ae}}\right)(s_0^+)^2\right]^2\right|. \quad \text{(II.3)}$$

Numerical investigation of this quantity has shown that $M < 1$ for all the Reynolds and Schmidt numbers for which results are reported here.

Résumé—Des réacteurs à écoulement turbulent avec des surfaces catalytiques isothermes bien définies fournissent une méthode pour obtenir les vitesses de processus de surface rapides. Cependant, même en écoulement turbulent, la diffusion tend à masquer le comportement véritable de la surface pour des conversions raisonnables d'espèces chimiques. Pour estimer l'effet de la diffusion sur la vitesse de réaction, le problème de Graetz pour l'écoulement turbulent entre des plaques parallèles avec une réaction du nième ordre sur une paroi a été résolu.

Les concentrations globales ont été obtenues dans une gamme de nombres de Reynolds de 30000 à 70000, de nombres de Schmidt de 0,2 à 1,0, d'ordres de réaction de 1,0 à 2,0 et de constantes de vitesse de réaction de zéro à l'infini. Les nombres de Nusselt entièrement établis étaient approximativement proportionnels à la puissance 0,75 du nombre de Reynolds et à la puissance 0,65 du nombre de Schmidt pour les cas contrôlés par la diffusion. Les nombres de Nusselt entièrement établis dépendaient aussi un peu de la vitesse de réaction.

Zusammenfassung—Chemische Reaktoren mit turbulenter Strömung entlang genau definierter katalytischer Oberflächen ermöglichen ein Verfahren zur Bestimmung von sich schnell ändernden Oberflächenprozessen. Aber selbst bei turbulenter Strömung führt die Diffusion zu einer Verschleierung des wirklichen Oberflächenverhaltens bei entsprechenden Umwandlungen chemischer Stoffe. Zur Abschätzung des Einflusses der Diffusion auf die Reaktionsgeschwindigkeit wurde das Graetz–Problem für turbulente Strömung zwischen parallelen Platten bei einer Reaktion n-ter Ordnung an einer Wand gelöst.

Mischkonvektionen wurden im Reynolds–Bereich 30000 bis 70000, bei Schmidt–Zahlen von 0,2 bis 1,0, Reaktionsordnungen von 1,0 bis 2,0 und Reaktionsgeschwindigkeitskoeffizienten von Null bis Unendlich erhalten. Für diffusionsbestimmte Fälle waren die voll ausgebildeten Nusselt–Zahlen angenähert proportional der Potenz 0,75 der Reynolds–Zahl und der Potenz 0,65 der Schmidt–Zahl. Die voll ausgebildeten Nusselt–Zahlen erwiesen sich auch etwas abhängig von der Reaktionsgeschwindigkeit.

Аннотация—Турбулентные реакторы с изотермическими каталитическими поверхностями позволяют развить метод получения скоростей быстрых процессов, происходящих на поверхности. Однако, даже в турбулентном потоке диффузия маскирует истинное поведение поверхности при значительных превращениях химических веществ.

Чтобы оценить влияние диффузии на скорость реакции, решена задача Гретца для турбулентного течения между параллельными пластинами при наличии реакции «*n*-го порядка» на одной стенке.

Средние объемные концентрации получены для диапазона чисел Рейнольдса 30000–70000, чисел Шмидта 0,2–1,0, порядков реакций 1,0–2,0 и постоянных скоростей реакции, варьируемых от нуля до бесконечности. Числа Нуссельта для полностью развитого течения приближенно пропорциональны числу Рейнольдса в степени 0,75 и числу Шмидта в степени 0,65 для случаев контролируемой диффузии. Числа Нуссельта для полностью развитого потока также несколько зависят от скорости реакции.